The 14th International Congress on the Chemistry of Cement

Proceedings

Beijing • China, October 2015

Photocatalytic performance of calcium aluminate cements modified with TiO_2

Pérez-Nicolás, M.[1], Navarro-Blasco, I.[1], Duran, A. [1], Sirera, R. [1], Fernández, J.M.[1], Alvarez, J.I.[1*]

1. MIMED Research Group, Department of Chemistry and Soil Sciences, University of Navarra, 31008 – Pamplona, Spain

Abstract

The photocatalytic activity of powdered TiO_2 (75% anatase, 25% rutile) was tested after the incorporation of the additive in mortars of calcium aluminate cement. Two different CACs were used according to their chemical and mineralogical composition: one of the CAC was a high alumina cement (H-CAC, 70.9% of Al_2O_3) while the other one was a low alumina cement (L-CAC, 42.0% of Al_2O_3) with a large amount of ferrite. One batch of the prepared mortars was tested after being subjected to 28 days under a normal curing regime (20ºC and 95% RH). A second batch was tested after a curing regime of 60ºC and 100% RH (for 24 hours) and then 20ºC and 95% RH. This second curing regime intended to induce the conversion reaction, which is responsible for the formation of stable calcium aluminate hydrates at the expense of metastable hydrates. Different properties such as workability, setting time and compressive strength were determined in the tested mortars in order to study the influence of the TiO_2 addition. The photocatalytic effect was assessed by means of the NO_x abatement under UV irradiation. The TiO_2-H-CAC mortars were found excellent systems to decrease NO_2 concentrations in connection with the more abundant presence of aluminates. The better NO_2 retention improved the NO_x removal. An chemical interaction between ferrite and TiO_2 was suggested to take place in the L-CAC mortars as evidenced by XRD, SEM, EDAX and zeta potential analyses. This interaction originated two new iron titanate phases, namely pseudobrookite and, to a lesser extent, ilmenite. The reduced band-gap energy of these compounds compared with that of TiO_2 improved the photocatalytic efficiency of L-CAC samples in the visible spectrum, as proved by Methyl Orange degradation tests, conferring a self-cleaning ability to the TiO_2-bearing iron-reach L-CAC under visible illumination.

Originality

Although CAC is used in many building as well as industrial structures, its modification upon addition of photocatalytic additives has not yet been addressed and that is precisely the purpose of the present work. We intend to obtain for the first time depolluting CAC mortars modified with different amounts of TiO_2. The effect of the TiO_2 incorporation on setting time, compressive strength and mineralogical composition of the CAC mortars will be assessed. PCO efficiency of these TiO_2-bearing CAC mortars will be also measured by means of the NO_x abatement. The modified depolluting mortars could be then applied in different tunnels, industrial floors and urban areas in which CACs are usually applied.

***Keywords**: Calcium Aluminate Cement; X-ray Diffraction; Compressive Strength; NOx abatement.*

*** Corresponding author: jalvarez@unav.es, Tel +34 948 425600, Fax +34 948 425647**

1. Introduction

The presence in the air of nitrogen oxides NO_x is one of the causes of the atmospheric pollution. It has been recognised as one of the most serious environmental problems (Beevers, S.D., *et al*, 2012). NO_x are one of the most common gaseous pollutants in the urban atmosphere being very injurious to the human health. Many adverse environmental effects like acid rain and ozone depletion are caused by their presence in the earth atmosphere. For that reason, is essential to find of ways to remove the NO_x from the atmosphere. One possibility is the use of photochemical oxidation (PCO) assisted processes which have gained a great attention to promote the degradation of inorganic toxic gases and organic pollutants. These processes are related - although not only- to the use of TiO_2 and the combinations thereof (Di Paola, A., *et al*, 2012.).

These powdered photocatalysts should be immobilized in order to improve practical applications. This immobilization provides surfaces that can be reached by light irradiation. One type of matrix that is useful to this aim comprises binding materials under condition that (i) present low degree of chemical interaction with photocatalyst particles; (ii) exhibit stability in the face of products formed; (iii) provide enough surface area to guarantee an adequate level of photocatalytic reaction; and (iv) are environmentally friendly.

Previous works show that these photocatalytic agents have been successfully included in Portland Cement (PC) creating better materials not only with depolluting properties but also with self-cleaning ability of their surfaces (Chen, J.; *et al, 2011)* (Folli, A., *et al,* 2012). A widespread distribution of the active agent is achieved with the incorporation of photocatalysts into cement materials and, if it is applied to outdoor exposed surfaces large enough, could be helpful in urban environments to reduce the contaminants level. On the other hand, the self-cleaning capacity safeguards the aesthetic characteristics and at the same time minimizes the maintenance and cleaning expenses (Smits, M., *et al,* 2014).

The PCO of NO_X occurs through the following reactions (Sugrañez, R.; *et al,*2013):

$$TiO_2 + h\nu \rightarrow e^- + h^+ \quad (1)$$

$$H_2O + h^+ \rightarrow H^+ + OH\bullet \quad (2)$$

$$O_2 + e^- \rightarrow O_2\bullet^- \quad (3)$$

$$NO + O_2\bullet^- \rightarrow NO_3^- \quad (4)$$

$$NO + OH\bullet \rightarrow HNO_2 \quad (5)$$

$$HNO_2 + OH\bullet \rightarrow NO_2 + H_2O \quad (6)$$

$$NO_2 + OH\bullet \rightarrow NO_3^- + H^+ \quad (7)$$

A certain degree of erosion of the PC mortars (Ibusuki, T., 2010) has been described because the acids formation (reactions 5 and 7) after the NOx capture on the surface of the mortars in the form of alkaline nitrate (reaction 7). Moreover it has been reported that during the photocatalytic process (reaction 6) some amounts of NO_2 were produced and were not retained by the PC system. These amounts of released NO_2 partially counteract the photocatalytic efficiency (Sugrañez, R.; *et al,*2013) (Cárdenas, C., *et al,* 2012).

One type of cement is calcium aluminate cement (CAC) which is principally made of monocalcium aluminate (CA) and with different proportions of $C_{12}A_7$, C_5A_3, C_3A and C_4AF. The interest in CACs is continuously growing because of their rapid hardening and enhanced durability properties (Juenger, M.C.G., *et al,* 2011). The purpose of this work is the modification of CACs upon addition of TiO_2, which novelty lies on the fact that there is a lack

in the literature. The photocatalytic performance of these new mortars under UV irradiation as well as under visible light irradiation was studied.

2. Experimental section

2.1. Materials

Mortars were prepared by using two types of CAC. One of the CACs was low alumina cement (L-CAC) with 17.0 wt. % in Fe_2O_3, and the other one contains high alumina percentages (H-CAC) with only a 0.1 wt. % in Fe_2O_3.

The mineralogical composition of these cements as proved by XRD was: for L-CAC, XRD studies revealed a main phase $CaAl_2O_4$ (CA) and minor phases with iron such as Ca_2FeAlO_5 (C_4AF), $Ca_3TiFe_2O_8$ and FeO; for H-CAC, the X-ray diffraction studies showed as main phases $CaAl_2O_4$, (CA) and $CaAl_4O_8$ (CA_2) and a minor phase of $Ca_{12}Al_{14}O_{33}$ ($C_{12}A_7$) with negligible amounts of iron-bearing compounds. L-CAC and H-CAC were supplied by Ciments Molins and Kerneos. CAC cements were mixed with a normalized siliceous aggregate. TiO_2 as photocatalyst (Aeroxide P25, Evonik, 75% anatase and 25% rutile) was added. To ensure a good workability of the samples, a polycarboxylate-based superplasticizer (Melflux2651^e, BASF) was used.

2.2. Methods

2.2.1. Obtaining of the mortars

Weight ratios of 1:3 and 1:0.37 were used, respectively, for cement:aggregate and cement:water relationships. TiO_2 percentages with respect to cement of 1%, 3%, 5% and 10 wt.% were added. Different amounts of the superplasticizer were required ranging from 0.07% to 2.5% for L-CAC mortars and from 0.10% to 1.10% for H-CAC mortars.

Additives, aggregate and CAC were mixed for 10 min at low speed in a blender. Later water was added and mixed at low speed for 90 s. Then fresh state properties were determined. Lastly, cylindrical mortars samples were prepared in 36x40 mm cylindrical casts and de-moulded 24 h later. Normal curing condition (20°C and 95% RH) was imposed to half of the samples and the second curing condition (hereinafter, forced curing condition), with high temperatures and RH (60°C and 100% RH, and after 24h, 20°C and 95% RH) to the rest of the samples. Samples subjected to normal curing condition were expected to develop metastable phases, while the forced curing condition was applied in order to provoke stable cubic aluminate hydrates formation. Samples were cured for 28 days and three samples of each mortar were tested.

2.2.2. Characterization

Consistency and setting time were studied as fresh properties. After the curing period, compressive strengths were measured at a loading rate of 50 $N \cdot s^{-1}$. Pore size distributions (PSD) were obtained by mercury intrusion porosimetry (Micromeritics-AutoPoreIV-9500; pressure 0.0015 to 207 MPa). Mineralogical characterization by X-ray diffraction (XRD) was done in a Bruker D8 ($CuK_{\alpha 1}$, from 2º to 80º 2θ; increment of 0.02º at 1 step.s^{-1} scan rate).

Textural characteristics and elemental compositions of the samples were performed by a Zeiss DSM-940A SEM coupled with an EDAX probe.

2.2.3. Photocatalytic studies: NO_x oxidation and organic dyes degradation

In NO_x oxidation tests a irradiated with a xenon lamp (Solarbox 3000) with an irradiance of 25±1 $W \cdot m^{-2}$ adjusted by a Delta-Ohm HD-2101.1 photoradiometer, with a LP-471 probe (315-400 nm) and a laminar-flow reactor and were used. Conditions were 50±10% RH and

25±2ºC. The photoreactor (300 mL) was fed by a 1000 ppb NO stream. The residence time of NO in the photoreactor was ca. 4 s. Concentrations of NO and NO_2 were determined by chemiluminescence (Environnement AC32M) at a 3.0 $L \cdot min^{-1}$ flow.

The sample was in the dark for 10 min with NO_x stream flowed over it. Then, the photoreactor was irradiated for 30 min. Neither NO_x adsorption on mortar surface nor direct photolysis evidences were found.

For organic dyes degradation studies, cylindrical samples (36x10 mm) were coated with 1 mL of aqueous Methyl Orange (MO) solution (0.1 $g \cdot mL^{-1}$). The area exposed was limited to 19.23 cm^2 discs and irradiated with a Philips LED (irradiance 10±1 $W \cdot m^{-2}$ between 400 and 700 nm).in the absence of UV radiation. Data were collected at 12, 24, 48 and 72 hours. CIELab coordinates were registered by a Konica-Minolta spectrophotometer CR-300. Colour coordinates were brightness (L), range between red to green (a) and range from blue to yellow (b), according to the Commission Internationale de l'Eclairage[21], where ΔE, which served to estimate the total variation of color, is:

$$\Delta E = L^2 + a^2 + b^2$$

The higher ΔE variation, the larger the discoloration of MO.

3. Results and discussion

3.1. Properties of tested mortars

It has been observed that the higher amount of photocatalytic additive in mortars the higher demand in water because of the small particle size of the TiO_2. Furthermore, the higher the amount of photocatalyst, the larger was the percentage of superplasticizer.

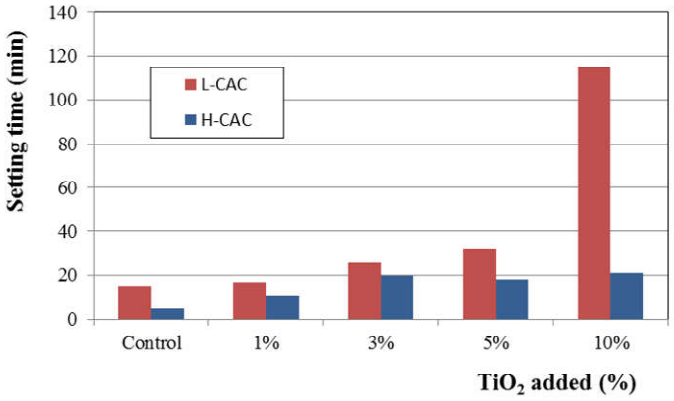

Figure 1 Setting time values of the different %TiO_2 loaded L- and H- CAC mortars.

Data collected in Figure 1 shows how incorporation of TiO_2 caused a setting time delay. An example of that is: 0%-CAC samples displayed a setting time of 15 min (L-CAC) or 5 min (H-CAC), while 3 wt.% TiO_2-bearing L-CAC and H-CAC samples showed setting times of 26 and 20 min, respectively. Presence of significant amounts of superplasticizer in the fresh mixtures (10 wt.% TiO_2) contributed in a larger extent to the delay in the setting time (Jansen, D., *et al,* 2012) The high alumina cement, H-CAC shows the shortest setting times in comparison with the low alumina cement, L-CAC. This fact can also be ascribed to the faster hydration of calcium aluminates as compared with the hydration of the ferrite phase ($Ca_2(Al_xFe_{1-x})_2O_5$). Ferrite phase is the main characteristic cementitious phase that is present in large amount in the L-CAC. While this phase is absent in the H-CAC, it is undoubtedly identified in the L-CAC. To sum up, mortars with both cement types presented short setting

times in comparison with PC (Sant, G., *et al,* 2008) so the induced delays did not imply significantly negative consequences for their application.

All the tested mortars containing TiO_2 showed acceptable mechanical resistance for certain practical applications, showing compressive strengths larger than 20 MPa (Fig. 2). Samples cured under normal curing condition (Fig. 2) commonly displayed greater compressive strengths than those subjected to forced curing condition (Fig. 3). This fact can be connected with the conversion reaction between hexagonal metastable phases and cubic stable phases. Cubic stable phases (mainly hydrogarnet, C_3AH_6, and gibbsite, AH_3) are denser hydrates than hexagonal metastable phases and the formation of the former results in a porosity increase and a subsequent strength decrease.

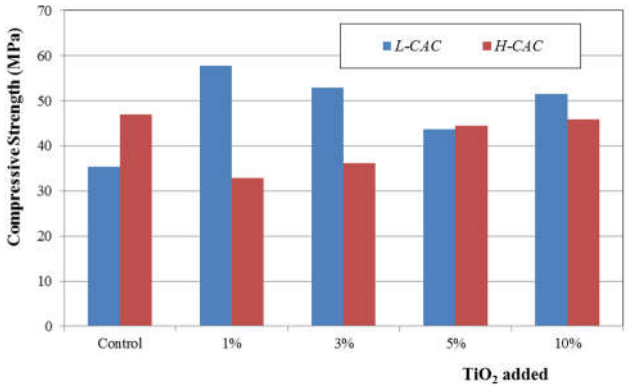

Figure 2 Compressive strength values of L- and H-CAC mortars loaded with different percentages of TiO_2 cured at 20°C and 95% RH for 28 days.

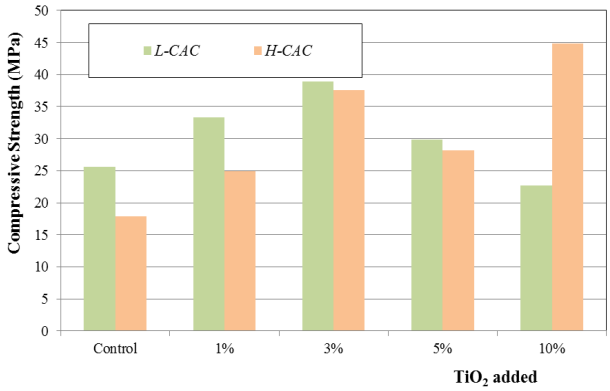

Figure 3 Compressive strength values of L- and H-CAC mortars loaded with different percentages of TiO_2 cured at 60°C and 100% RH for 24 h.

Pore size distributions and XRD examinations demonstrated these assertions. Metastable compounds (CAH_{10} and C_2AH_8) together with some remaining anhydrous compounds (CA and $C_{12}A_7$ –mayenite-) were identified by XRD studies in samples under normal curing condition. On the other hand, in samples under forced curing condition, stable aluminate hydrates, hydrogarnet (C_3AH_6) and gibssite (AH_3), were evident (Fig. 4).

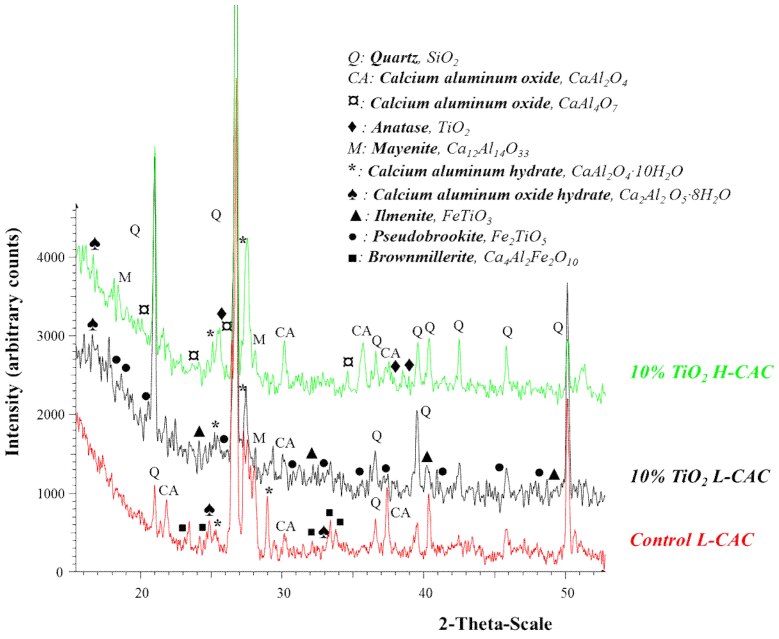

Figure 4. Comparative XRD profiles of 10 %TiO_2 loaded L- and H- CAC mortars cured at 20°C and 95% RH for 24 h.

H-CAC plain samples after normal curing condition showed greater mechanical resistance values than L-CAC plain samples. This fact can be a result of the hydration of calcium aluminates, the main responsible compounds for the early mechanical resistance. H-CAC samples contain a greater amount of calcium aluminates (70.9 wt.% content of Al_2O_3 and 28.0 wt.% of CaO) as compared with the lower one of L-CAC (42.0 wt.% content of Al_2O_3 and 37.8 wt.% of CaO), which also presented an exceptional amount of ferrite. The presence of ferrite does not contribute to the strength due to its short- term hydration.

XRD studies of H-CAC showed the absence of any new distinct crystalline phase involving TiO_2, indicating that no strong chemical interaction took place upon addition of the TiO_2 in these samples. In 10 wt. % TiO_2-loaded H-CAC sample, the anatase peaks were identified. Nevertheless, for L-CAC samples, the diffraction peak of anatase almost completely disappeared. At the same time, the diffraction peaks of the ferrite (brownmillerite) phase – which could be observed in a plain L-CAC sample – underwent a clear reduction in the TiO_2-bearing L-CAC sample. Whereas the appearance of pseudobrookite (Fe_2TiO_5) was identified by its diffraction peaks at 17.9, 18.2, 25.6, 32.8, 36.6 and 37.4º 2θ, and, to a lesser extent, the presence of ilmenite ($FeTiO_3$) was also found (main diffraction peaks at 32.4, 35.1, 48.8 and 24.0º 2θ). The finding of this mixture of iron titanates was a good indicative of the interaction between TiO_2 and ferrite of the L-CAC. The substitution of Ti^{4+} by Fe^{3+} was favoured in our experimental conditions thanks to the closeness of their respective ionic radii (0.64 and 0.67 Å).

In the present work, our experimental evidences for L-CAC helped us to find a clear interaction TiO_2-ferrite, although there is some controversy on this topic so far (Chen, J., *et al* 2009).

In Fig.5 micrographs of CACs samples under normal curing condition can be seen. Plain L-CAC samples as well as H-CAC samples present similar textural appearance (with fractured surfaces and with some well identified compounds, such as hexagonal plate-like crystals of

C_2AH_8 metastable calcium aluminates (Navarro-Blasco, I., *et al*, 2013), in good agreement with the XRD results.

The addition of 5 wt.% of TiO_2 resulted in a different micro-morphology depending on the type of cement: for L-CAC samples irregular and non-geometric aspect were seen with some ill-defined clusters, under normal curing regime. Nevertheless, SEM studies let us see prismatic crystals with well-defined structures in H-CAC samples.

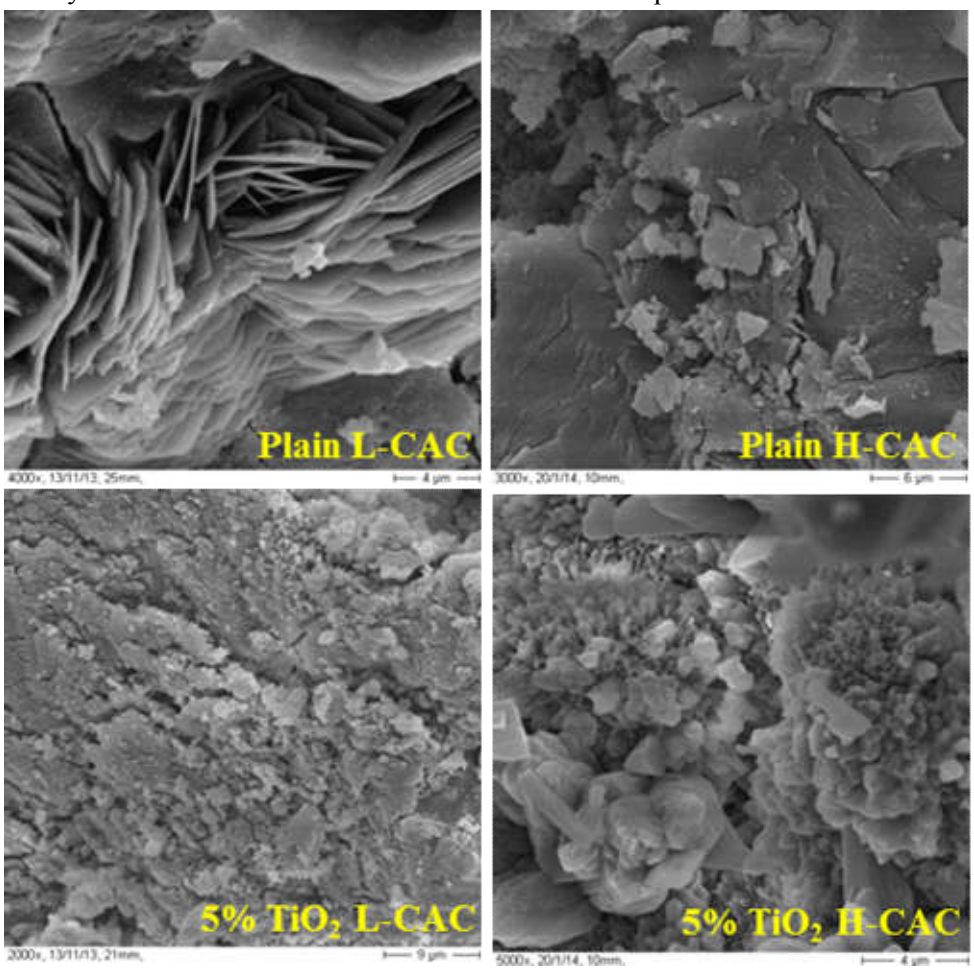

Figure 5 SEM micrographs of free- and 5wt.%- TiO_2 CAC samples after curing at 20°C and 95% RH for 24 h.

We can conclude that, in H-CAC samples, there is no interaction and TiO_2 seems to be physically entrapped in the matrix of the cement. Therefore, H-CAC, with more amount of TiO_2 available to oxidize NO_x, should achieve better photocatalytic efficiencies than L-CAC samples.

3.2. Measurement of the photocatalytic efficiency of the mortars under UV and visible light irradiation

Figure 6 and 7 show the profiles of NO, NO_2 and NO_x abatement measurements (UV irradiation) for samples with 1, 3 and 5 wt.% TiO_2 by weight of L-CAC and H-CAC, respectively. The NO and NO_x profiles have three common stages: i) During the first 10 minutes, when the irradiation source was off, neither the activation of the sites of TiO_2 on the surface of photocatalytic mortars nor NO oxidation took place. NO concentration remained constant. ii) The heterogeneous photocatalytic reaction took place under UV radiation (next 30 min) beginning the oxidation of pollutants by means of (1) to (7) reactions. NO

concentration was decreasing until reached a plateau. iii) UV radiation was off during the last 10 min of the test and consequently the NO concentration reverted to its initial value. Conversely to Portland cement, in general, the NO_2 gas profile decreased under UV radiation.

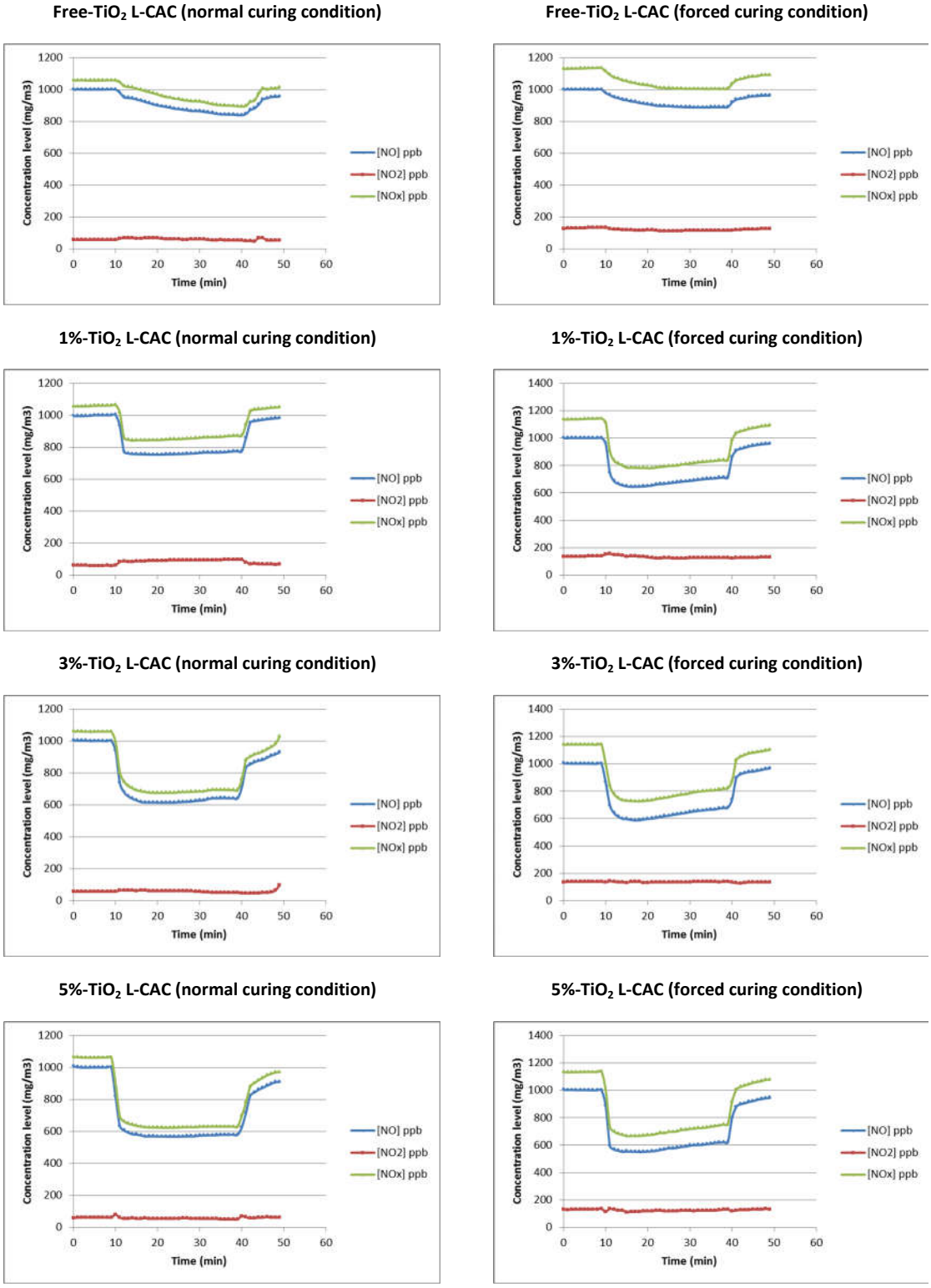

Figure 6. Conversion charts of the NO, NO_2 and NO_x abatement of different TiO_2 loaded L-CAC samples after normal curing at 20°C and 95% RH (left) and forced curing 60°C, 100% RH (right side).

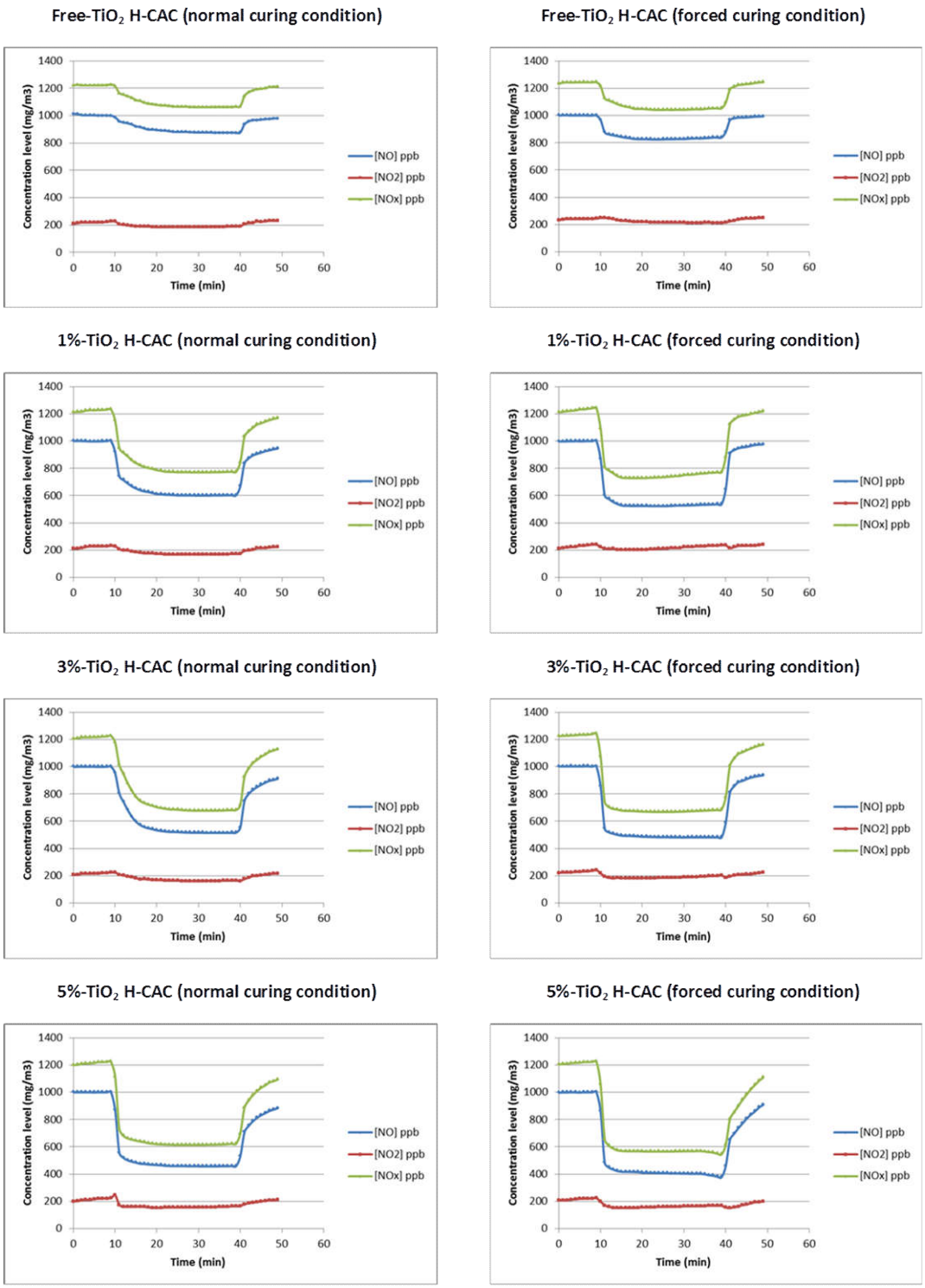

Figure 7. Conversion charts of the NO, NO_2 and NO_x abatement of different TiO_2 loaded H-CAC samples after normal curing at 20°C and 95% RH (left side) and forced curing at 60°C and 100% RH (right side).

The removal rate (%) of NO is a very interesting parameter to assess the specific efficiency of each mortar in the PCO. Removal rate of NO values are collected in Table 1. It can be observed that the higher the dosage of additive, the higher the NO abatement. Maximum values of NO conversion (65%) were seen for 10wt.% TiO_2 in H-CAC. The same amount of

photocatalytic additive in L-CAC yielded up to 48% of abatement. In the present study we could observe that even for large amounts of additive (10 wt.%), CACs behave as an appropriate matrix to immobilize important amounts of photocatalyst. This fact does not agree with several previous works dealing with Portland cement matrices, which had reported that a TiO_2 upload over ca. 2wt.% produced an inversion of the photocatalytic efficiency (Lucas, S.S., *et al,* 2013) based on the recombination of electon-hole pair in an excess of TiO_2.

Table 1. The NO removal rate (%) obtained for L-CAC and H-CAC samples with different TiO_2 content and subjected to different curing conditions.

	TiO_2 (%)	L-CAC	H-CAC
Normal curing condition	Control	16	14
	1%	39	40
	3%	25	49
	5%	44	54
	10%	48	55
Forced curing condition	Control	11	18
	1%	36	48
	3%	42	52
	5%	45	62
	10%	48	65

If the samples are subjected to the mild hydrothermal conditions under forced curing regime, we can study the evolution (conversion reaction from metastable hexagonal hydrates to cubic stable phases) of the CAC samples over time. Thanks to the values of the NO conversion measured under both curing conditions it can be concluded that this unavoidable conversion will not have a negative effect on the photocatalytic activity.

NO_2 fixation (data gathered in Table 2) is as important as NO conversion during the PCO process. Even though the strong decomposition of NO_2 by TiO_2 photocatalytic-based compounds is well known, previous studies revealed that NO_x abatement in Portland cements produced an increase of the NO_2 concentration due to the fast photochemical oxidation of NO (Sugrañez, R.; *et al,*2013) (Cárdenas, C., *et al,* 2012). The values obtained in the present work prove that CACs are excellent materials in order to achieve a suitable NO_2 fixation. For example H-CAC samples reduced the amount of NO_2 twice as much as L-CAC samples, both with the same amount of photocatalyst (10 wt.% TiO_2). Threefold NO_2 amount was removed by 10 wt.% of TiO_2 H-CAC samples in comparison with the value obtained for L-CAC samples, subjected to forced curing condition. As shown in Table 2, the percentage contribution of the NO_2 conversion to the total percentage of NO_x removal was commonly higher in H-CAC than in L-CAC samples.

Table 2 Contribution ratio (%) of NO_2 abatement related to the total degradation of NO_x

TiO_2 (%)	L-CAC 20ºC 95% RH	L-CAC 60ºC 100% RH	H-CAC 20ºC 95% RH	H-CAC 60ºC 100% RH
Control	11.7	16.7	26.1	17.3
1%	11.7	8.6	13.5	7.5
3%	13.6	3.2	11.7	10.4
5%	6.4	5.0	14.6	10.6
10%	7.7	6.1	12.6	13.7

The significant efficiency of NO_2 sorption and ulterior conversion can be explained by the chemical composition of the cementitious matrix of the CACs. We hypothesize that UV illumination produces holes on calcium aluminates that would act as Lewis acids sites upon

which NO_2 (Lewis base) can then interact. This kind of interaction has been described in other photocatalytic systems (Devahasdin, S., *et al,* 2003) including some barium aluminates (Akiti Jr., *et al,* 2001), calcium aluminates (Proto, A., *et al,* 2013) and alkaline-earth metal oxides (CaO, MgO and BaO) that have been seen able to adsorb NO_2 (in order to increase the NO_2 removal). In addition, some divalent metal aluminates (e.g. $MgAl_2O_4$ and $ZnAl_2O_4$) with structures similar to calcium aluminates are used as wide band-gap semiconductors sensitive to UV illumination (Ragupathi, C., *et al,* 2013).

The differences in the NO_2 conversion (Table 2) observed between the TiO_2-free samples of H-CAC and L-CAC are related to their different chemical composition: the lower NO_2 degradation capacity measured for L-CAC are based in the lower amount of calcium aluminates of L-CAC in comparison with H-CAC.

On the other hand, Table 1 shows a better NO removal for H-CAC samples than for L-CAC samples. The reaction between ferrite phase and TiO_2, which gives rise to pseudobrookite and ilmenite, contributes to explain the lower efficiency of L-CAC of the NO conversion under UV irradiation. This fact is a consequence of the more reduced band-gaps and lower PCO activity of the resulting pseudobrookite (Ye, F.X., *et al,* 2008) (2.18 eV) and ilmenite (Ye, F. and Ohmori, A., 2002) (2.58 eV), together with a reduction of active sites of the titania surface. It is, however, necessary, to consider that a certain amount of TiO_2 do not react with ferrite in TiO_2-bearing L-CAC samples, consequently this amount of TiO_2 will take part in the NO conversion of these samples.

Based on the observed formation of iron titanates in L-CAC samples, we expected that the use of these mortars should result in improved photocatalytic efficiency under visible light. As a matter of fact, it had been reported that coupling titania with semiconductors (among them mixtures Fe_2O_3-TiO_2) with a narrow band gap widened its sensitivity towards the visible spectrum. Bearing that in mind, comparative tests of organic dyes degradation under visible light irradiation were carried out on L-CAC and H-CAC samples. It should be noticed that plain L-CAC samples initially showed a marked MO degradation value, as an expected consequence of the amount of iron oxides present, which by themselves are able to photodegradate organic dyes. Plotted values were normalized with respect to each one of the plain cement samples (as control groups) in order to discard the contribution of the plain cements (in terms of differences in chemical composition as well as in as pore size distribution) and of the photolytic self-degradation of the dyes. Figure 8 depicts the normalized values for the degradation of MO under visible light irradiation, as measured by ΔE (chromatic alteration of the surface of the mortars). The response was quasi-dosage-dependent and was lower for H-CAC than for L-CAC samples. In spite of the wide-gap of the TiO_2 present, the observation of a certain degradation of dyes in H-CAC mortars can be related to a photosensitized pollutant degradation mechanism, in which the dye acted as a sensitizer of the photocatalyst. It must be considered that the depicted values were the net contribution of the additive, since the base values of the plain mortars had already been subtracted in the normalization process. The dose-response effect was larger for L-CAC than for H-CAC. The larger values of MO degradation obtained in L-CAC samples confirmed the activity of the pseudobrookite in the visible wavelengths, whereas the activity in the UV region (measured by NO_x degradation) can be related to the TiO_2 remaining unreacted and ilmenite presence. This behaviour is a first indication of a good self-cleaning ability of these

TiO_2-modified iron-rich L-CAC mortars under visible light.

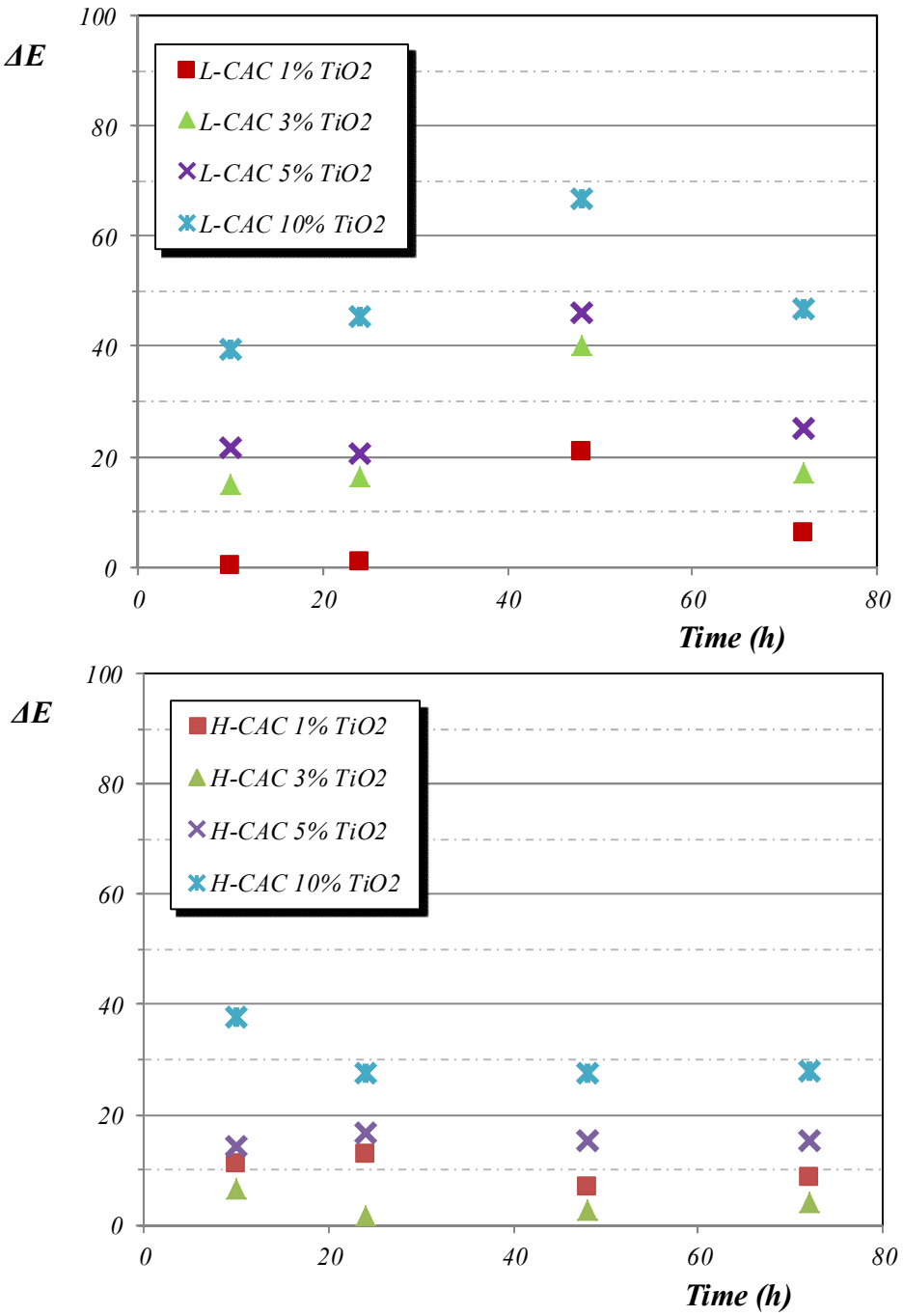

Figure 8. Color variation of methyl orange-treated samples under visible light irradiation in: a) TiO_2-doped L-CAC and b) TiO_2-doped H-CAC samples. Normal curing regime. All plotted values were normalized with respect to the response of control samples (photocatalyst-free samples).

Overall, the CAC-based mortars exhibited a very remarkable NO_x removal rate thanks to the good efficiency in the NO and NO_2 conversion. Best values were obtained for H-CAC samples. Comparatively, under similar experimental conditions, a lower NO_x conversion was reported for Portland cement-based pastes with 3.5% of TiO_2 (Folli, A., *et al,* 2012). This fact gives assurance of the effectiveness of TiO_2-modified CACs as depolluting materials to be used in many practical applications, such as tunnels, industrial floors and urban areas.

4. Conclusions

Calcium aluminate cements, modified by incorporation of different percentages of TiO_2, have been successfully identified as depolluting materials for NO_x reduction. The TiO_2 presence gives rise to mortars with significant compressive strengths over 20 MPa.

Two different calcium aluminate cements have been studied (high and low alumina cements). An interaction between the ferrite (brownmillerite) phase present in the L-CAC with the TiO_2 added, is the responsible of the formation of certain amounts of titanates, mainly pseudobrookite.

For 10 wt.% TiO_2 L-CAC and H-CAC mortars, NO oxidation rates ca. 48% and 65% were observed, respectively. Values obtained for L-CAC mortars are ascribed to the presence of iron titanates with a smaller band-gap than that of TiO_2.

CAC matrices are proved to be suitable to immobilize large amounts of photocatalytic additives when important conversions values of NO are required. This fact is seen in the excellent PCO performance even for samples containing 10 wt. % of TiO_2.

Conversion of metastable hydrates into cubic stable hydrates is provoked under forced curing condition. This fact does not make the photocatalytic efficiency to decline, so that the long-term PCO activity is assured.

Higher values of MO degradation (under visible light) for L-CAC samples when compared with those obtained for H-CAC, showed the activity of the new phase formed (pseudobrookite) by the reaction between TiO_2 and ferrite in the L-CAC samples. This fact confirms that TiO_2 doped with iron could be an efficient photocatalyst under visible light.

Calcium aluminates matrices are excellent materials in order to sorb NO_2 as compared with other binding materials. Consequently, NO conversion rates will be increased by using CACs.

5. Acknowledgments

The authors want to thank Ciments Molins and Kerneos España for the material supplied. This work was funded by Fundación Universitaria de Navarra (grant FUNA2013-15108402) and by Fundación CajaNavarra (under grant 31-2014). M. Pérez also gratefully acknowledges Friends of University of Navarra Inc. for a pre-doctoral grant.

6. References

Akiti Jr., *et al,* 2001. Development of an advanced calcium-based sorbent for desulfurizing hot coal gas. *Advances in Environmental Research*, 5, 1 31-38.

Beevers, S.D., *et al*, 2012. Trends in NOx and NO2 emissions from road traffic in Great Britain. *Atmospheric Environment*, 54, 0 107-116.

Cárdenas, C., *et al,* 2012. Functionalized building materials: Photocatalytic abatement of NOx by cement pastes blended with TiO2 nanoparticles. *Construction and Building Materials,* 36, 0 820-825.

Chen, J.; *et al, 2011*. Photocatalytic cement-based materials: Comparison of nitrogen oxides and toluene removal potentials and evaluation of self-cleaning performance. *Building and Environment,* 46, 49 1827-1833.

Devahasdin, S., *et al,* 2003. TiO2 photocatalytic oxidation of nitric oxide: transient behavior and reaction kinetics. *Journal of Photochemistry and Photobiology A: Chemistry,* 156, 1–3 161-170.

Di Paola, A., *et al*, 2012. A survey of photocatalytic materials for environmental remediation. *Journal of Hazardous Materials*, 3-29, 0 211–212.

Folli, A., *et al,* 2012. TiO_2 photocatalysis in cementitious systems: Insights into self-cleaning and depollution chemistry. *Cement and Concrete Research*, 42, 3 539-548.

Ibusuki, T., 2010. Cleaning Atmospheric Environment (Photocatalytic activities of TiO2), In Photocatalysis: Science and Technology. Springer: Berlin Heidelberg.

Jansen, D., *et al,* 2012. Change in reaction kinetics of a Portland cement caused by a superplasticizer — Calculation of heat flow curves from XRD data. *Cement and Concrete Research* 42, 2 327-332.

Juenger, M.C.G., *et al,* 2011. Advances in alternative cementitious binders. *Cement and Concrete Research,* 41, 12 1232-1243.

Lucas, S.S., *et al,* 2013. Incorporation of titanium dioxide nanoparticles in mortars — Influence of microstructure in the hardened state properties and photocatalytic activity. *Cement and Concrete Research,* 43, 0 112-120.

Management. Eds.; Politecnico di Milano, Centro per la Conservazione e Valorizzazione dei Beni Culturali: Milano.

Navarro-Blasco, I., *et al*, 2013. A novel use of calcium aluminate cements for recycling waste foundry sand (WFS). *Construction and Building Materials,* 48, 0 218-228.

Proto, A., *et al,* 2013. Ca-based adsorbents for NOx measurement in atmospheric environments surrounding monumental and archeological sites, In Built Heritage 2013 Monitoring Conservation

Ragupathi, C., *et al,* 2013. Catalytic properties of nanosized zinc aluminates prepared by green process using Opuntia dilenii haw plant extract. *Chinese Journal of Catalysis,* 34, 10 1951-1958.

Sant, G., *et al,* 2008. Rheological properties of cement pastes: A discussion of structure formation and mechanical property development. *Cement and Concrete Research,* 38, 11 1286-1296.

Smits, M., *et al,* 2014, July. Effect of process parameters on the photocatalytic soot degradation on self-cleaning cementitious materials. *Catalysis Today*, DOI: 10.1016/j.cattod.2013.10.001.

Sugrañez, R.; *et al,*2013. Enhanced photocatalytic degradation of NOx gases by regulating the microstructure of mortar cement modified with titanium dioxide. *Building and Environment,* 69, 0 55-63.

Suttiponparnit, K., *et al,* 2011. Role of surface area, primary particle size, and crystal phase on titanium dioxide nanoparticle dispersion properties. *Nanoscale Research Letters* 6, 27 1-8.

Ye, F. and Ohmori, A., 2002. The photocatalytic activity and photo-absorption of plasma sprayed TiO2–Fe3O4 binary oxide coatings. *Surface and Coatings Technology*, 160, 1 62-67.

Ye, F.X., *et al,* 2008. Dependence of photocatalytic activity on the compositions and photo-absorption of functional TiO2–Fe3O4 coatings deposited by plasma spray. *Materials Science and Engineering: B*, 148, 1–3 154-161.